Available online at www.sciencedirect.com
SCIENCE DIRECT
Catalysis Today 116 (2006) 391–399
CATALYSIS TODAY
www.elsevier.com/locate/cattod

Selective CO oxidation over $Ce_XZr_{1-X}O_2$-supported Pt catalysts

J.L. Ayastuy *, M.P. González-Marcos, A. Gil-Rodríguez, J.R. González-Velasco, M.A. Gutiérrez-Ortiz

Group of Chemical Technologies for Environmental Sustainability, Department of Chemical Engineering, Faculty of Sciences, Universidad del País Vasco/Euskal Herriko Unibertsitatea, P.O. Box 644, 48080 Bilbao, Spain

Available online 14 July 2006

Abstract

CO oxidation on $Pt/Ce_XZr_{1-X}O_2$ ($X = 0$, 0.15, 0.5, 0.68, 0.8 and 1) was studied, both in the absence of H_2 and in H_2-rich streams. Catalyst activity was correlated with support reducibility and Pt content. A certain excess of oxygen ($\lambda > 1$) with respect to CO had to be fed to the system in order to obtain complete CO conversion in the presence of H_2. Three catalysts were found capable of complete CO depletion with effective oxygen use at $\lambda = 2$: $Pt/Ce_{0.8}Zr_{0.2}O_2$, $Pt/Ce_{0.68}Zr_{0.32}O_2$ and $Pt/Ce_{0.5}Zr_{0.5}O_2$. More demanding working conditions, by increasing GHSV from 12,000 up to 18,000 h^{-1}, reduced the adequate catalysts to just two: $Pt/Ce_{0.68}Zr_{0.32}O_2$ and $Pt/Ce_{0.5}Zr_{0.5}O_2$, and only the latter would be adequate if the conditions were still more demanding. The presence of CO_2 and H_2O, produced a general decrease of CO conversion for the catalysts supported on mixed oxides and, among them, only $Pt/Ce_{0.5}Zr_{0.5}O_2$ remained capable of complete CO removal with effective oxygen use at $\lambda = 2$. However, the presence of CO_2 and H_2O increases CO conversion of Pt/CeO_2 such that this catalyst arises as an alternative. Choice between Pt/CeO_2 and $Pt/Ce_{0.5}Zr_{0.5}O_2$ requires further research, and may depend on the actual application.

Keywords: CO oxidation; Selective CO oxidation; Ceria-zirconia mixed oxides; PROX; Pt catalysts

1. Introduction

Hydrogen for PEMFC could be produced by means of a fuel reformer, which should be followed by water gas shift reaction (WGSR) in order to remove bulk CO [1,2]. So as to prevent PEMFC stack electrodes deactivation, additional CO removal is necessary to reduce CO content down to 10 ppm [3]. For this purpose, selective CO oxidation reaction or preferential oxidation reaction (PROX) is the most promising, cost-effective and effective (in the sense of H_2 consumption) method [4–7].

PROX reaction removes low levels of CO from H_2-rich gas streams by reacting with molecular oxygen. Process parameter $\lambda = 2 \times P_{O_2}/P_{CO}$ defines the oxygen excess with respect to stoichiometric amount to oxidize CO. As H_2 oxidation competes with CO oxidation in such a system, the catalyst must show high activity and selectivity towards CO oxidation. As the selectivity is inversely proportional to oxygen content, an ideal catalyst should be active even with low oxygen contents (low λ values), in order to maintain selectivity at acceptable values. Due to the gas composition in the PROX inlet stream, WGS and methanation reactions could also occur.

Noble metal supported on alumina has been proposed as ideal catalyst for PROX reaction [5–11]. Pt-based catalysts are reported to be robust oxidation catalysts [12,13]. Oxidation of CO on alumina-supported noble metal catalysts is known to take place via a single-site competitive Langmuir–Hinshelwood mechanism. These catalysts are characterized by operating at high temperatures and needing high oxygen excess for complete depletion of CO, with the corresponding lack of selectivity. However, they are resistant to deactivation by water [7], although slightly inhibited by CO_2 [14]. Formulation of new, highly active catalysts in the low temperature range (80–100 °C) is a decisive step, because the selectivity of such catalysts would be enhanced with respect to that of catalysts active in the high temperature range (170–200 °C).

Extremely fine deposited gold particles have been reported to be very active at very low temperatures [15–19]. However, they showed to be very sensitive to the presence of CO_2 and

* Corresponding author. Tel.: +34 94 6012619; fax: +34 94 6015963.
E-mail address: joseluis.ayastuy@ehu.es (J.L. Ayastuy).

0920-5861/$ – see front matter © 2006 Elsevier B.V. All rights reserved.
doi:10.1016/j.cattod.2006.05.074

steam. Mixed CuO-ceria have been also reported as powerful catalysts for PROX reaction [14,20], as well as zeolite-based [21] and bimetallic catalysts of Pt-Sn [22,23].

New Pt-based catalyst formulations are being developed towards supplying catalysts with an additional site for oxygen activation, which will enhance the reaction rate. In this sense, Pt-based catalysts promoted with Fe [24–28], ceria [29] or Co [30] have been reported in the literature. Pt supported on ceria catalysts are reported to be very active oxidation catalysts due to the redox properties of ceria [31]. Also, ceria-based supports have been studied for PROX reaction. Ceria presents very high oxygen storage capacity (OSC) [32], which is very helpful for oxidation on reductive environments, with the cyclic incorporation/removal of structural oxygen. CeO_2 has multiple effects on catalysts, such as: (a) promotion of metal dispersion, (b) promotion of CO oxidation by employing lattice oxygen and (c) storage and release of oxygen [33]. Addition of ZrO_2 enhances the OSC capacity of CeO_2 by increasing the oxygen vacancies of the support due to the high oxygen mobility in the solid solution formed [34–37].

Wootsch et al. [38] studied a series of $Pt/Ce_XZr_{1-X}O_2$ catalysts and found they are very active in the 80–100 °C range. Roh et al. [39] have also studied Pt supported on ceria-zirconia mixed oxide catalysts and found they are very active even at 60 °C, the most active being the 80% ceria-20% zirconia support.

In this work, a series of $Pt/Ce_XZr_{1-X}O_2$ ($X = 0, 0.15, 0.5, 0.68, 0.8$ and 1) catalysts has been tested for CO oxidation both in H_2-free and H_2-rich environments. The effect of feeding 5% CO_2 and 5% H_2O in the feedstream on CO oxidation behaviour has been studied, and activities, selectivity towards CO oxidation and CO yield, have been calculated. The effect of spatial time on catalyst activity and selectivity has also been studied.

2. Experimental

2.1. Catalysts preparation

A series of $Pt/Ce_XZr_{1-X}O_2$ ($X = 0, 0.15, 0.5, 0.68, 0.8$ and 1) catalysts was prepared by impregnating the supports (Rhodia) with an aqueous solution of tetraamminplatinum(II) nitrate (Aldrich). After impregnation, the samples were dried overnight at 110 °C, and then calcined in air at 400 °C for 5 h. Catalyst particle size in the range 0.16–0.25 mm was used in the experiments. Prior to experiments, catalysts were activated in situ by flowing 100 $cm^3\ min^{-1}$ of an equimolecular mixture of H_2 and He for 3 h at 300 °C.

2.2. Catalysts characterization

Actual platinum content of catalysts was evaluated by atomic absorption spectroscopy (AAS). BET specific surface area and pore size distribution were determined for the supports by N_2 adsorption at −196 °C. Platinum dispersion was calculated from H_2 chemisorption at 0 °C (Micromeritics ASAP 2010), assuming an H/Pt stoichiometry of 1/1 for irreversibly adsorbed H. Platinum particle size has been estimated by assuming spherical cluster geometry.

Both support and catalyst structure was characterized by X-ray powder diffraction (Philips Xpert-MPD), using Cu Kα radiation, with typical operation parameters being: a scanning 2θ range of 20–90° with 2° min^{-1} scanning rate and 0.02° data interval. Crystallite sizes were estimated from the integral breadth of the line with the highest intensity using the Scherrer's equation.

TPR experiments (Micromeritics Autochem 2910) were carried out from −30 °C until 900 °C for the supports and 400 °C for the catalysts, with a heating rate of 10 °C min^{-1} in a flow of 50 $cm^3\ min^{-1}$ of 5% H_2 in Ar, after pretreating the sample by heating to 150 °C (1 h) in a flow of nitrogen, in order to remove surface water, followed by heating up to the final temperature to be reached in the TPR (either 900 or 400 °C), in order to clean the sample surface, an then cooling down to −30 °C. The exhaust gases were detected by a TCD and recorded.

2.3. Reactor setup, analysis method and calculations

Experiments were carried out in a plug flow reactor, with total bed volume of 1 cm^3. Helium was used as an inert gas during the experiments. Reactant gases were analytical-grade H_2, CO_2, O_2 and a calibrated mixture of 10.5% Ar in CO. When required, ultra pure water (Millipore) was added by means of a Bronkhorst Hitec mass flow controller followed by evaporation to the gas mixture. All experiments were carried out with a total flow rate of 200 $cm^3\ min^{-1}$ (GHSV = 12,000 h^{-1}) except when the effect of spatial time was analysed, with the following compositions: 1% CO, 0–60% H_2, 0.5–1% O_2, 0–5% CO_2, 0–5% H_2O and He to balance, λ ranging between 1 and 2. Catalytic tests were carried out at atmospheric pressure, in a temperature ramp of 3 °C min^{-1} from 25 to 225 °C (from 50 to 225 °C when water was fed to the reactor).

Analysis of reactor feedstream and products was carried out by MS (Hewlett-Packard 5973). As no methane formation and neither forward nor reverse WGS reaction was observed during the experiments, CO conversion (X_{CO}) was calculated based on the CO consumption within the reactor. Similarly, oxygen conversion (X_{O_2}) was calculated based on the oxygen consumption within the reactor. Selectivity (S) of oxygen towards CO rather than H_2 was calculated, in streams with H_2, as the ratio between oxygen consumed to oxidize CO and total oxygen consumption. By combination of X_{CO}, λ and X_{O_2}, we can obtain the following relationship:

$$S\,(\%) = \frac{100}{\lambda} \times \frac{X_{CO}}{X_{O_2}} \tag{1}$$

Catalyst efficiency, defined as CO yield, was calculated as $S \times X_{CO}$, and given as a percentage.

3. Results and discussion

3.1. Support and catalyst characterization

Table 1 summarizes characteristics of all catalysts. BET surface area of mixed oxides ranged around 100 $m^2\ g^{-1}$, while pure ceria and zirconia were 164 and 57 $m^2\ g^{-1}$, respectively.

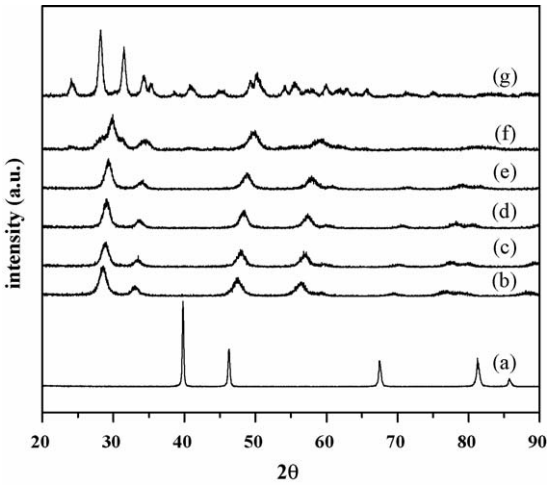

Fig. 1. Powder XRD patterns for $Ce_XZr_{1-X}O_2$ supports calcined in air at 550 °C for 4 h: (b) $X = 1$ (pure CeO_2), (c) $X = 0.8$, (d) $X = 0.68$, (e) $X = 0.5$, (f) $X = 0.15$ and (g) $X = 0$ (pure ZrO_2). The pattern corresponding to Pt is also shown (a).

Pure ceria and pure zirconia showed the lowest and the highest mean pore diameter, respectively. Mean pore diameter increased with zirconia content in the mixed oxides, which is related to the structural changes occurring when Zr^{4+} substitutes Ce^{4+} [40].

X-ray diffraction patterns of $Ce_XZr_{1-X}O_2$ supports are presented in Fig. 1. Except for $X = 0.15$, addition of ZrO_2 to CeO_2 did not result in segregated phases. However, ceria most intense peak was shifted to significantly higher diffraction angles with increasing Zr content, which agrees with the results reported by Hori et al. [41]. This observation was attributed to the replacement of Ce^{4+} cation by the smaller radius Zr^{4+} cation, with the correspondent shrinking of the lattice. For $Ce_{0.15}Zr_{0.85}O_2$ support, the main ceria peak at 29.8° overlaps with zirconia peaks at 28.2° and 31.5°, which suggests formation of a segregated zirconia phase and a Ce–Zr solid solution. The Pt diffractogram was obtained by calcination of $Pt(NH_3)_4(NO_3)_2$ in air, at 400 °C for 5 h. Five sharp and symmetric peaks could be detected at $2\theta = 39.8°$, 46.3°, 67.5°, 81.2° and 85.7°, the peak relative intensities being 100, 57, 47, 49 and 31, respectively. These peaks could be attributed to reflexions of Pt(1 1 1), Pt(2 0 0), Pt(2 2 0), Pt(3 1 1) and Pt(2 2 2), respectively, from metallic Pt (cubic phase) (JCPDS 88-2343 file). No peaks from platinum oxide were detected.

Addition of zirconia to ceria does not substantially modify particle size, which is between 6.5 and 8.0 nm.

X-ray diffraction patterns of $Pt/Ce_XZr_{1-X}O_2$ catalysts were identical to those of $Ce_XZr_{1-X}O_2$ supports, i.e., no Pt signal was detected in the patterns. This could be explained by the high Pt dispersion in all the samples, and the subsequent low Pt particle diameter (Table 1), which is below the detection limit for XRD, combined with the low catalyst platinum content.

As shown in Fig. 2a, TPR profile of pure ceria showed two peaks, at 490 and 834 °C, suggesting that reduction of ceria occurs in two steps. The former peak is associated to hydrogen consumption in the reduction of surface ceria while the latter is associated to reduction of bulk ceria [31,42]. On the other hand, pure ZrO_2 showed no peak in the −30 to 900 °C temperature range. TPR profiles of the mixed oxides showed essentially a main broad peak centered at 530–540 °C, which is shifted towards higher temperature when zirconia content increases, and another broader peak, less defined, centered at 710–780 °C, which is shifted to lower temperature when Zr content increases. Several authors have also observed the shift of the low temperature maximum for mixed oxides as Zr content was increased [42–44].

TPR hydrogen uptake for the supports up to 600 °C is given in Table 1. It has been associated to support reducibility. While H_2 uptake of ceria agrees reasonably well with that associated to surface reduction (about 4 μmol m^{-2}), H_2 uptake of the mixed oxides is much higher than that needed for reduction of surface ceria (zirconia is not reduced). This fact has been associated to reduction of several layers in the bulk of the mixed oxide, due to improved mobility of lattice oxygen produced by distortion of the mixed oxide lattice induced by incorporation of Zr into cubic ceria [33]. Thus, reduction of the solid is extended into the bulk.

Table 1
Characteristics of $Pt/Ce_XZr_{1-X}O_2$ ($X = 0$, 0.15, 0.5, 0.68, 0.8 and 1) catalysts

Catalyst	BET[a] ($m^2\ g^{-1}$)	V_P[b] ($cm^3\ g^{-1}$)	d_P[c] (nm)	d_S[d] (nm)	Supports H_2 uptake[e] (μmol g^{-1})	Pt[f] (%)	D[g] (%)	d_{Pt}[h] (nm)	Catalysts H_2 uptake[i] (μmol g^{-1})
Pt/CeO_2	164	0.19	4.0	6.9	530	0.54	71.5	1.3	50
$Pt/Ce_{0.8}Zr_{0.2}O_2$	103	0.18	4.8	8.0	996	0.32	58.8	1.6	98
$Pt/Ce_{0.68}Zr_{0.32}O_2$	101	0.24	7.0	7.8	1290	0.27	63.3	1.5	134
$Pt/Ce_{0.5}Zr_{0.5}O_2$	99	0.21	6.4	6.5	1320	0.16	85.7	1.1	142
$Pt/Ce_{0.15}Zr_{0.85}O_2$	97	0.26	8.7	7.4	510	0.25	54.0	1.7	53
Pt/ZrO_2	57	0.24	13.5	14.0	~0	0.16	81.6	1.2	2

[a] For supports.
[b] Pore volume for supports.
[c] Mean pore diameter for supports.
[d] Crystallite size for supports.
[e] From H_2–TPR data for supports, up to 600 °C.
[f] Metal content of the catalysts in wt%.
[g] Metal dispersion, from H_2 chemisorption data.
[h] Mean Pt particle size.
[i] From H_2–TPR data for catalysts, up to 400 °C.

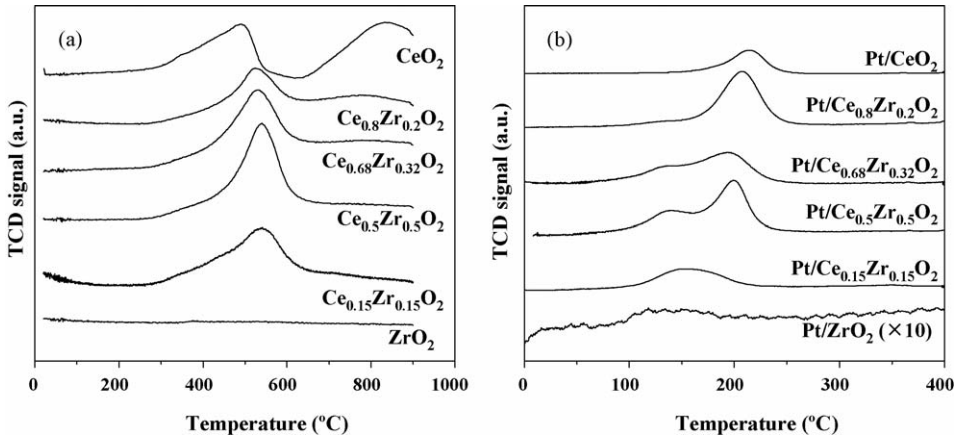

Fig. 2. H_2–TPR profiles for $Ce_XZr_{1-X}O_2$ supports (a) and $Pt/Ce_XZr_{1-X}O_2$ catalysts (b). The Pt/ZrO_2 profile has been magnified 10 times.

Fig. 2b shows TPR profiles for $Pt/Ce_XZr_{1-X}O_2$ catalysts up to 400 °C. Pt/ZrO_2 catalyst showed very low hydrogen uptake, with a maximum at 159 °C probably associated to Pt (the profile for this sample has been 10 times magnified in the figure). TPR profile for Pt/CeO_2 catalyst in the 0–400 °C temperature range presented a single peak at 214 °C. Except for catalyst with $X = 0.15$, all $Pt/Ce_XZr_{1-X}O_2$ catalysts, showed a main peak around 200 °C accompanied by a shoulder around 150 °C. $Pt/Ce_{0.15}Zr_{0.85}O_2$ catalyst showed a single peak at 153 °C. Comparison between TPR profiles for corresponding supports and catalysts showed an important promotion in the reduction of the support due to Pt metal, with a significant shift of the peaks to lower temperatures. H_2 uptake for the catalysts up to 400 °C has been also included in Table 1. Comparing the two columns in Table 1, we can see that the ratio of H_2 uptake between supports and their corresponding catalysts in the low temperature range remains similar ($Pt/Ce_{0.5}Zr_{0.5}O_2 \approx Pt/Ce_{0.68}Zr_{0.32}O_2 > Pt/Ce_{0.8}Zr_{0.2}O_2 > Pt/Ce_{0.15}Zr_{0.85}O_2 \approx Pt/CeO_2 \gg Pt/ZrO_2$), being mainly a function of the reducibility of the support.

3.2. Activity tests

3.2.1. CO oxidation reaction in H_2-free stream

Prior to selective CO oxidation, the ability of $Pt/Ce_XZr_{1-X}O_2$ catalysts for CO oxidation in a H_2-free stream was studied. The light-off curves for all catalysts at $\lambda = 2$ are shown in Fig. 3. It is worth to notice that all supports were also checked in the same conditions, and no significant activity was observed below 200 °C, which agrees with the observation of Thammachart et al. [44].

The activity of catalysts containing ceria with $X = 0.8$, 0.68 and 0.15 in pure CO oxidation is very similar, slightly higher than that of pure ceria, as shown in Fig. 3. The catalyst with $X = 0.50$ shows the lowest activity of the ceria-containing series, while catalyst with pure zirconia is, by far, the less active. Ignition temperature, T_{Ig} (related to the CO onset temperature and calculated as the temperature of maximum slope in CO conversion versus temperature plot), and temperature for complete CO conversion, T_{100}, for all catalysts are summarized in Table 2. T_{Ig} values are very similar for most ceria-containing catalysts, in the range 69–76 °C, except for catalyst with $X = 0.5$, which is increased to 103 °C. The T_{Ig} for Pt/ZrO_2 catalyst is the highest, 171 °C. The same trend was observed in T_{100}. For all ceria-containing catalysts (except for $X = 0.5$, which is shifted to 112 °C) T_{100} ranged between 75 and 86 °C. Again, catalyst with pure zirconia requires the highest temperature for complete CO depletion, 179 °C operating with $\lambda = 2$.

According to the values in Table 2, we can expect all ceria-containing catalysts studied to be active for CO oxidation in H_2-rich environment in the temperature range of operation of a PEMFC, i.e., 75–100 °C, while Pt/ZrO_2 catalyst is not expected to be active below 150 °C (in the same range than Pt/Al_2O_3 [45]). The different behavior has been related to the presence of ceria in the support, and its ability to supply structural oxygen through reduction. In catalysts without ceria (or a reducible support), CO oxidation takes place via a typical Langmuir–Hinshelwood mechanism where both CO and O_2 are adsorbed onto Pt. The presence of ceria (or a reducible support) adds a second reaction pathway, Mars–Van Krevelen type, by supplying atomic oxygen from its structure. Considering that supports without Pt presented no activity below 200 °C, this second mechanism must take place in the Pt–support interface,

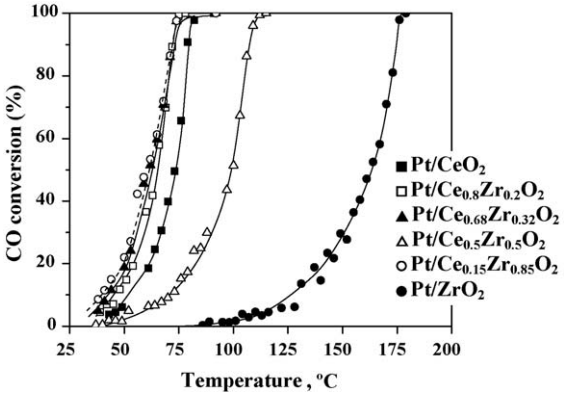

Fig. 3. CO oxidation light-off curves for $Pt/Ce_XZr_{1-X}O_2$ catalysts in H_2-free streams ($\lambda = 2$).

Table 2
T_{Ig} and T_{100} for pure CO oxidation, and T_{Ig} for CO oxidation in hydrogen-rich stream, at λ = 2, for $Pt/Ce_XZr_{1-X}O_2$ (X = 0, 0.15, 0.5, 0.68, 0.8 and 1) catalysts

Catalyst	Without H_2		With H_2
	T_{Ig} (°C)	T_{100} (°C)	T_{Ig} (°C)
Pt/CeO_2	76	81	67
$Pt/Ce_{0.8}Zr_{0.2}O_2$	69	75	64
$Pt/Ce_{0.68}Zr_{0.32}O_2$	71	86	68
$Pt/Ce_{0.5}Zr_{0.5}O_2$	103	112	88
$Pt/Ce_{0.15}Zr_{0.85}O_2$	71	86	85
Pt/ZrO_2	171	179	161[a]

[a] Not reached, T_{max} given instead.

where CO is adsorbed on Pt and oxygen supplied by the support. The presence of ceria in the support has been reported to favour oxygen activation by spillover in the Pt–support interface [46], which agrees with our observations.

This second pathway could be expected to be favoured by the reducibility of the catalyst, a measurement of which is given by the H_2 uptake of the catalysts in Table 1. According only to this effect, the predicted catalytic activity would be: $Pt/Ce_{0.5}Zr_{0.5}O_2 \approx Pt/Ce_{0.68}Zr_{0.32}O_2 > Pt/Ce_{0.8}Zr_{0.2}O_2 > Pt/Ce_{0.15}Zr_{0.85}O_2 \approx Pt/CeO_2 \gg Pt/ZrO_2$. Comparing this prediction with the results of Fig. 3, catalyst Pt/CeO_2 and mainly $Pt/Ce_{0.5}Zr_{0.5}O_2$ present lower activity than expected. However, other aspects should be considered. In the case of Pt/CeO_2, the lower activity is easily explained if we consider that the value of H_2 uptake in Table 1 is proportional to the specific surface area for a given support composition. Thus, it is a good measurement of reducibility of the solid to compare among samples with similar specific surface area, like the catalysts supported on the mixed oxides, but overestimates it for a sample with much higher specific surface area, like the ceria used in this work. With $Pt/Ce_{0.5}Zr_{0.5}O_2$ the low activity can be related to the much lower Pt content in this catalyst than the other ceria-containing catalysts (see Table 1).

Concerning the similar behaviour of $Pt/Ce_{0.8}Zr_{0.2}O_2$, $Pt/Ce_{0.68}Zr_{0.32}O_2$ and $Pt/Ce_{0.15}Zr_{0.85}O_2$, it can be associated with working in oxidising conditions, where the oxygen supply is not the limiting rate, but that of CO.

3.2.2. CO oxidation reaction in H_2-rich stream: selective CO oxidation

3.2.2.1. Feed free from CO_2 and H_2O. All $Pt/Ce_XZr_{1-X}O_2$ catalysts were checked for CO oxidation in streams containing high H_2 concentration (60 vol.%). CO conversion, selectivity and CO yield curves with temperature for all catalysts, at λ = 2, are shown in Fig. 4. By comparison of Figs. 3 and 4, it is noticeable that, except for $Pt/Ce_{0.15}Zr_{0.85}O_2$ and Pt/ZrO_2, CO conversion curves are shifted to lower temperature in the presence than in the absence of hydrogen. In order to facilitate comparison, T_{Ig} values obtained in the experiments with H_2-rich feedstreams have been included in Table 2. Also, in the absence of H_2, CO conversion increased with temperature until complete conversion was attained, while in the presence of H_2, CO conversion increases with temperature until a maximum value is attained ($X_{CO_{max}}$), not necessarily complete conversion,

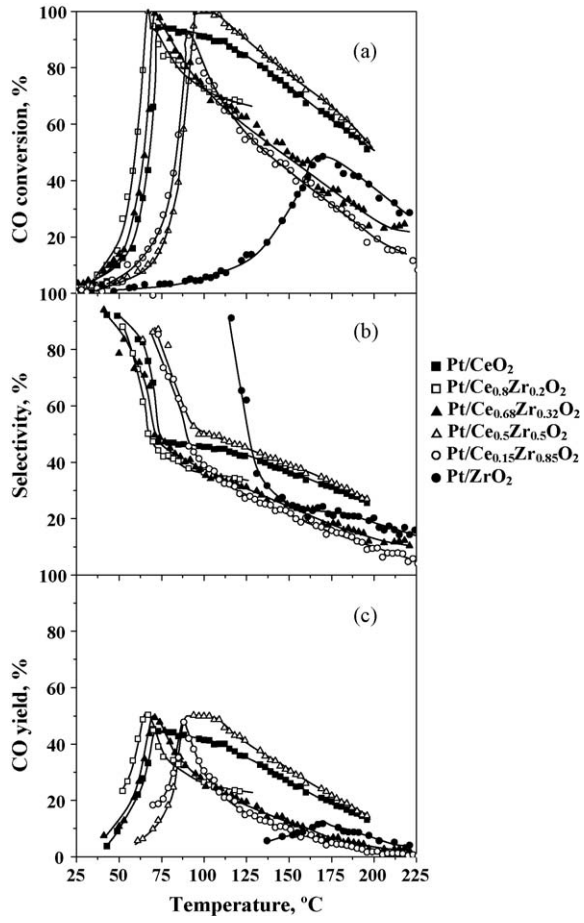

Fig. 4. CO conversion (a), selectivity (b) and CO yield (c) in hydrogen-rich streams for $Pt/Ce_XZr_{1-X}O_2$ catalysts.

and from that temperature (T_{max}) CO conversion decreases with temperature.

The presence of hydrogen produces two main effects in the system: it changes the reaction environment to highly reducing while adding a reactant in competition with CO for the O_2, which would negatively affect CO conversion; and adds a component in competition with CO for the Pt adsorption sites, which may positively affect CO conversion at low temperature by inhibiting the known self-poisoning effect of CO on Pt surface.

Thus, it seems that the former effect predominates in catalysts with low or no ceria content in the support, while the latter predominates when $X \geq 0.5$. The values of T_{max}, $X_{CO_{max}}$ and their correspondent selectivity (S_{max}) and CO yield ($(S{\cdot}X_{CO})_{max}$), corresponding to the experiments in Fig. 4, are shown in Table 3 (λ = 2). Except for Pt/ZrO_2, where maximum CO conversion is below 50%, comparison between T_{100} in Table 2 and T_{max} in Table 3 (λ = 2) gives a clear indication of the temperature shift produced by the presence of H_2. Catalysts with X = 0.68 and 0.5 showed the highest shift, 15 °C, those with X = 1 and 0.8 showed a lower difference, 8 °C, while those with X = 0.15 and 0 presented a shift in the opposite direction of 5 and (about) 10 °C, respectively. The beneficial effects of the capability of the support to provide oxygen are, then, more clear when the experimental conditions are more demanding.

Table 3
CO conversion, selectivity and CO yield ($S{\cdot}X_{CO}$) values corresponding to the optimum operation temperature (temperature for maximum CO conversion) in PROX reaction for λ = 1 and 2

Catalyst	λ = 1				λ = 2			
	T_{max} (°C)	$X_{CO_{max}}$ (%)	S_{max} (%)	$(S{\cdot}X_{CO})_{max}$ (%)	T_{max} (°C)	$X_{CO_{max}}$ (%)	S_{max} (%)	$(S{\cdot}X_{CO})_{max}$ (%)
Pt/CeO_2	91	56.7	56.7	32.1	73	94.4	47.2	44.5
$Pt/Ce_{0.8}Zr_{0.2}O_2$	71	70.8	70.8	50.1	67	100	50	50
$Pt/Ce_{0.68}Zr_{0.32}O_2$	71	77.3	77.3	59.8	71	99.4	49.7	49.4
$Pt/Ce_{0.5}Zr_{0.5}O_2$	127	55.9	55.9	31.2	97	100	50	50
$Pt/Ce_{0.15}Zr_{0.85}O_2$	90	69.1	69.1	47.7	91	91.6	45.8	41.9
Pt/ZrO_2	164	28.8	28.8	8.3	170	48.6	24.3	11.8

Activity and selectivity in PROX strongly depend on oxygen excess (λ). The higher the λ is, the higher the maximum CO conversion achieved, but the lower the selectivity. As CO yield is the product of both conversion and selectivity, the effect of λ is not defined, and depends on the catalyst. The objective would be to operate with the maximum possible CO yield while keeping CO exit concentration below the required specifications for H_2 to be used as feed in a PEMFC.

The effect of λ has been studied by performing the same experiments in the presence of H_2, but with a value of λ = 1, i.e., stoichiometric amount of oxygen with respect to CO. T_{max}, $X_{CO_{max}}$, S_{max} and $(S{\cdot}X_{CO})_{max}$ are shown in Table 3 for λ = 1. Maximum CO conversion and its correspondent selectivity are identical because oxygen conversion is complete for maximum CO conversion. Also, no catalyst can completely remove CO from the stream with λ = 1, the maximum CO conversion being 77.3%, achieved at 71 °C, with $Pt/Ce_{0.68}Zr_{0.32}O_2$. The decrease in $X_{CO_{max}}$ when λ decreases is related to competition between H_2 and CO for the scarce oxygen.

Decreasing the amount of oxygen from λ = 2 to 1 produces experimental conditions much more demanding, where the rate-limiting step will be the supply of oxygen. Because of that, most of the curves are shifted to higher temperatures when λ decreases. The shift to higher temperature when λ is reduced from 2 to 1 decreases in the following order: $Pt/Ce_{0.5}Zr_{0.5}O_2$ (30 °C) > Pt/CeO_2 (18 °C) > $Pt/Ce_{0.8}Zr_{0.2}O_2$ (4 °C) > $Pt/Ce_{0.68}Zr_{0.32}O_2$ (0 °C) ≈ $Pt/Ce_{0.15}Zr_{0.85}O_2$ (−1 °C) > Pt/ZrO_2 (about −6 °C). We can see that the two samples most affected by the change in λ are precisely those who presented a CO oxidation activity in H_2-free streams below the value predicted by H_2 uptake in Table 1. Both have the capacity to supply oxygen to the Pt–support interface limited: Pt/CeO_2 because it can supply less oxygen per unit surface area, and $Pt/Ce_{0.5}Zr_{0.5}O_2$ because lower amount of Pt means less amount of interface, at least for similar dispersion values. The shift to lower temperature observed with $Pt/Ce_{0.15}Zr_{0.85}O_2$ and mostly Pt/ZrO_2 are related to the reduction of the competence for the Pt adsorption sites (less O_2) in the Langmuir–Hinshelwood pathway, which is the only mechanism on Pt/ZrO_2 and is expected to have a significant contribution in these conditions on $Pt/Ce_{0.15}Zr_{0.85}O_2$ (little amount of ceria in the support).

Roh et al. [39] studied $Pt/Ce_XZr_{1-X}O_2$ catalysts with $X = 1$, 0.8, 0.2 and 0, with Pt content in the range 0.5–1 wt%, and found that, for constant Pt loading, activity decreases in the order $Pt/Ce_{0.8}Zr_{0.2}O_2 > Pt/CeO_2 > Pt/Ce_{0.2}Zr_{0.8}O_2 > Pt/ZrO_2$. They studied the effect of Pt loading in CO conversion curves, and concluded that a decrease of Pt loading from 1 to 0.5% produced a shift in T_{max} of about 10 °C to higher values, although $X_{CO_{max}}$ was not modified. These authors reported a maximum CO conversion of 80%, at 60 °C for 1% $Pt/Ce_{0.8}Zr_{0.2}O_2$ catalyst, operating with λ = 1, which agrees quite well with our results considering that the Pt loading of our catalysts is much lower. However, Wootsch et al. [38] found that Pt/CeO_2 was the most active catalyst, operating at 100 °C and λ = 2, compared to $Pt/Ce_{0.68}Zr_{0.32}O_2$, $Pt/Ce_{0.5}Zr_{0.5}O_2$ and $Pt/Ce_{0.15}Zr_{0.85}O_2$; surprisingly, they reported a very active Pt/ZrO_2 catalyst, which achieved 98% CO conversion at 100 °C.

From the point of view of applicability, it is important to note that three catalysts are able to reach complete CO conversion for λ = 2: $Pt/Ce_{0.8}Zr_{0.2}O_2$, $Pt/Ce_{0.68}Zr_{0.32}O_2$ and $Pt/Ce_{0.5}Zr_{0.5}O_2$. Concerning CO yield, the three catalysts present, within experimental error, the same maximum value: 50%. In fact, this is the maximum CO yield attainable when λ = 2 if oxygen is completely consumed (which is desirable), and occurs above T_{max}, and indicates that the catalysts operate in an optimal way, i.e., complete CO removal occurs with effective oxygen use.

Another important point to be considered is the range of temperature in which complete CO conversion is maintained, as it will affect the required precision of the temperature control during operation. Both $Pt/Ce_{0.8}Zr_{0.2}O_2$ and $Pt/Ce_{0.68}Zr_{0.32}O_2$ present a very narrow temperature range, a single point in fact, of complete CO conversion, conversion increases quickly with temperature until T_{max} and decreases again quickly at higher temperature, and only $Pt/Ce_{0.5}Zr_{0.5}O_2$ presents a significantly wide temperature range (about 10 °C). According to Roh et al. [39], this does not significantly change with Pt loading, but Pt loading could be used to shift the maximum to the more convenient temperature range. Increasing the stable conversion range would require the use of higher λ values, i.e., more excess of oxygen, with the associated reduction of CO yield.

We have also calculated activation energies for both CO and H_2 oxidation for all the catalysts, which are shown in Table 4, assuming the differential reactor approach. The results indicate that the activation energy for CO oxidation is much lower than that for H_2 oxidation for all catalysts, included Pt/ZrO_2 catalyst. This result explains the observed monotonic decrease of selectivity with temperature: the higher the temperature is, the higher the $(-r_{H_2})/(-r_{CO})$ ratio is [14,47]. This ratio is around

Table 4
Activation energies calculated for CO and H_2 oxidation reactions

Catalyst	E_a (kJ mol^{-1})		E_{aH_2}/E_{aCO}
	CO oxidation	H_2 oxidation	
Pt/CeO_2	97.3 ± 14.2	145.9 ± 19.2	1.50
$Pt/Ce_{0.8}Zr_{0.2}O_2$	112.5 ± 30.9	172.1 ± 84.8	1.53
$Pt/Ce_{0.68}Zr_{0.32}O_2$	59.9 ± 7.0	90.2 ± 18.4	1.51
$Pt/Ce_{0.5}Zr_{0.5}O_2$	50.0 ± 14.9	76.8 ± 17.9	1.54
$Pt/Ce_{0.15}Zr_{0.85}O_2$	67.9 ± 8.8	172.7 ± 52.4	2.54
Pt/ZrO_2	32.1 ± 3.8	127.0 ± 14.3	3.96

1.5 for ceria-containing catalysts, except for $Pt/Ce_{0.15}Zr_{0.85}O_2$ – which is 2.5 – and is around 4 for Pt/ZrO_2 catalyst, and can be an indication of the relative contribution of the Mars–Van Krevelen mechanism to CO oxidation.

We have not found activation energy values for PROX reaction on ceria-zirconia-supported Pt catalyst in the literature. For pure CO oxidation (no PROX) on ceria-supported Pt catalyst, however, activation energies in the range 70–91 kJ mol^{-1} have been reported [48,49]. For the selective CO oxidation on Au/Fe_2O_3 and Pt-Sn/C catalysts, reported activation energies for CO and H_2 oxidation were around 30 and 45 kJ mol^{-1}, respectively. Although the catalytic systems are different, the E_{aH_2}/E_{aCO} calculated ratio is also 1.5, what points to similar mechanism.

3.2.2.2. Effect of CO_2 addition. The effect of adding 5% CO_2 to the feedstream has also been studied, at $\lambda = 2$. As an example, CO conversion, selectivity and CO yield for the catalyst presenting the lowest T_{max} at $\lambda = 2$ ($Pt/Ce_{0.8}Zr_{0.2}O_2$), is shown in Fig. 5. Fig. 6 summarises results for all catalysts in the absence (white bars) and in the presence of 5% CO_2 (striped bars).

Fig. 5 shows that CO_2 in the feedstream affects X_{CO} for $Pt/Ce_{0.8}Zr_{0.2}O_2$ only slightly, with a general shift of the curve about 10 °C to higher temperature, and a slight enhancement of conversion in the high temperature region (above T_{max}), and at very low temperature. $X_{CO_{max}}$ decreases from 100 to 96.1%, and CO conversion and CO yield curves present a similar trend.

Fig. 6 shows that all catalysts present a very similar behaviour, with a certain increase in T_{max}, and a general decrease in $X_{CO_{max}}$, S_{max} and $(S{\cdot}X_{CO})_{max}$. In fact, the three latter parameters present the same trend for each catalyst. Concerning T_{max}, the most notorious shift to higher values corresponds to $Pt/Ce_{0.5}Zr_{0.5}O_2$ (from 97 up to 115 °C), followed by Pt/CeO_2 and Pt/ZrO_2, the former two already discussed in relation to lower Pt content and lower reducibility per unit surface area, respectively, which limit their capacity to respond to more demanding situations, and the latter without a reducible support. CO_2 seems to affect both Langmuir–Hinshelwood and Mars–Van Krevelen pathways, probably by altering the distribution of adsorbed products on Pt sites. At very low temperature, it clearly reduces CO self-poisoning effect, increasing X_{CO} (see Fig. 5).

Although T_{max} value for $Pt/Ce_{0.5}Zr_{0.5}O_2$ catalyst is the most negatively affected by CO_2 addition, neither $X_{CO_{max}}$, S_{max} nor $(S{\cdot}X_{CO})_{max}$ are affected, i.e., $Pt/Ce_{0.5}Zr_{0.5}O_2$ remains capable of completely removing CO from the H_2 stream with effective oxygen use for $\lambda = 2$ in the presence of CO_2. Again, the range of temperatures for effective operation of this catalyst can be regulated with Pt loading. Also, despite the temperature increase observed in X_{CO} with Pt/CeO_2 by the addition of CO_2, there is an increase in $X_{CO_{max}}$, S_{max} and $(S{\cdot}X_{CO})_{max}$ such that the catalyst becomes capable of removing CO from the H_2 stream with effective oxygen use with $\lambda = 2$.

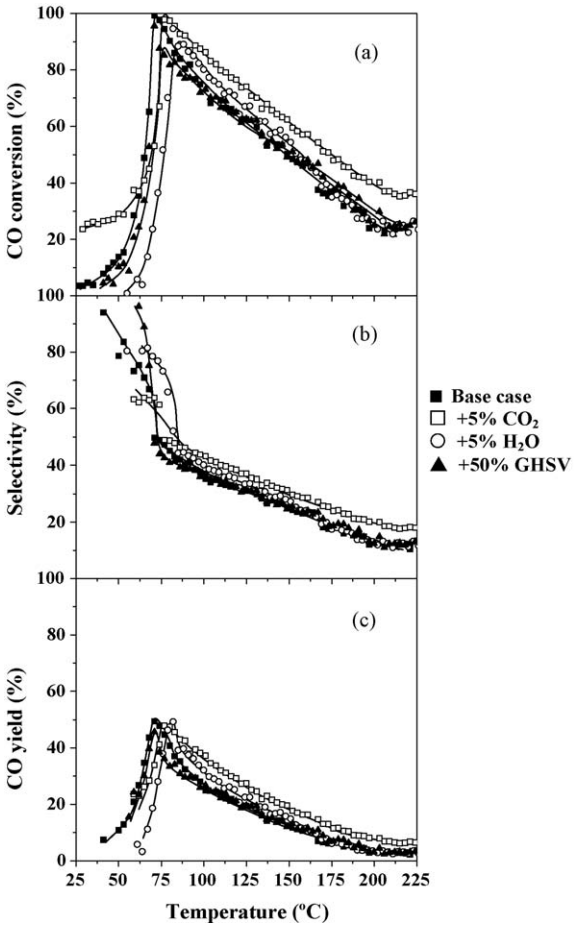

Fig. 5. Effect of the addition of 5% CO_2, 5% H_2O, and increasing the GHSV by 50%, on CO conversion (a), selectivity (b) and CO yield (c) for $Pt/Ce_{0.8}Zr_{0.2}O_2$.

Summarising, in the presence of 5% CO_2, both $Pt/Ce_{0.5}Zr_{0.5}O_2$ and Pt/CeO_2 catalysts are capable of completely removing CO with $\lambda = 2$.

3.2.2.3. Effect of H_2O addition. In the actual reformatted gas, there is a relatively high concentration of steam, which can affect catalyst activity and/or selectivity, as well as stability. Thus, $Pt/Ce_XZr_{1-X}O_2$ catalyst performance in PROX reaction when steam to a concentration of 5% is added to the feedstream was also evaluated, for $\lambda = 2$.

The effects observed by this addition on X_{CO}, selectivity and CO yield for $Pt/Ce_{0.8}Zr_{0.2}O_2$ are also shown in Fig. 5. In the low temperature region, the presence of steam clearly inhibits catalyst activity, whereas in the high temperature region activity

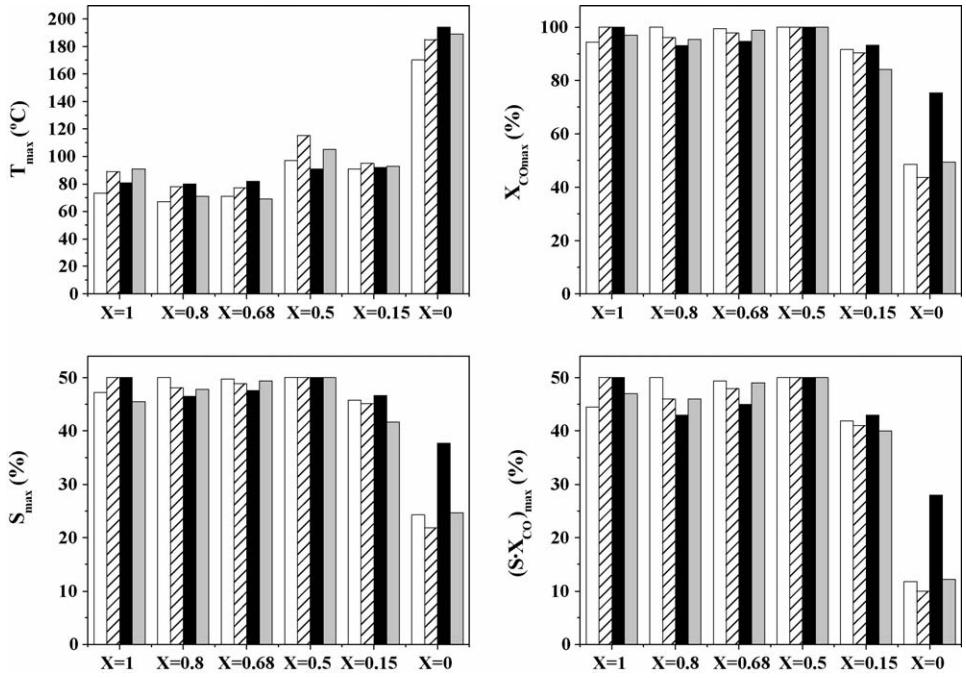

Fig. 6. Effect of the addition of 5% CO_2 (striped bars), 5% H_2O (black bars) and increasing the GHSV by 50% (grey bars), on T_{max}, $X_{CO_{max}}$, S_{max} and $(S{\cdot}X_{CO})_{max}$. White bars correspond to a feedstream free from CO_2 and H_2O, with a GHSV of 12,000 h^{-1} and $\lambda = 2$. X indicates ceria fraction in the support.

is not modified. T_{max} increases from 67 to 80 °C, while $X_{CO_{max}}$, S_{max} and $(S{\cdot}X_{CO})_{max}$ slightly decrease.

Fig. 6 summarises the results obtained by H_2O addition with all catalysts, for $\lambda = 2$ (black bars). We can see that the effect of steam addition to the feedstream depends on the catalyst composition, $X_{CO_{max}}$, S_{max} and $(S{\cdot}X_{CO})_{max}$ increasing except for catalysts $Pt/Ce_{0.8}Zr_{0.2}O_2$ and $Pt/Ce_{0.68}Zr_{0.32}O_2$. $X_{CO_{max}}$ for Pt/CeO_2 again reaches 100%. On the other hand, only $Pt/Ce_{0.5}Zr_{0.5}O_2$ presents a decrease in T_{max} with the addition of H_2O.

In summary, and keeping an eye on applicability, both $Pt/Ce_{0.5}Zr_{0.5}O_2$ and Pt/CeO_2 catalysts, and only them, are capable of complete CO removal from a H_2 feedstream with efficient oxygen use for $\lambda = 2$.

3.2.2.4. Effect of spatial time (GHSV). H_2 production on board in mobile devices requires continuous change in the rate of H_2 production to comply with variation of power requirements. It has been simulated by modifying the GHSV. In order to analyse the effect of spatial time on the catalyst performance in selective CO oxidation reaction, a total flow rate of 300 cm^3 min^{-1} (GHSV of 18,000 h^{-1}) was used. Fig. 5 shows the effects observed on $Pt/Ce_{0.8}Zr_{0.2}O_2$. T_{max} is practically unaltered (shifted 4 °C to higher values), and X_{CO}, selectivity and CO yield curves were coincident with those at 200 cm^3 min^{-1}.

The effect on all catalysts is shown in Fig. 6 (grey bars). Catalysts supported on pure oxides showed the most appreciable shift of T_{max} toward higher values (18 and 19 °C, for Pt/CeO_2 and Pt/ZrO_2, respectively), whereas it is almost unchanged for catalysts supported on mixed oxides. $X_{CO_{max}}$, S_{max} and $(S{\cdot}X_{CO})_{max}$ either remain constant or decrease with increasing GHSV for catalysts supported on the mixed oxides. Although a small increase in $X_{CO_{max}}$ for catalysts supported on pure oxides is observed when GHSV is increased (Fig. 6), it is not attributable to diffusion effects, but to conversion values corresponding to higher values of temperature (T_{max}).

Working with higher values of GHSV means more demanding conditions. This effect makes that the three catalysts originally able to effectively remove CO from the feedstream at $\lambda = 2$ and 12,000 h^{-1} in the absence of both CO_2 and H_2O ($Pt/Ce_{0.8}Zr_{0.2}O_2$, $Pt/Ce_{0.68}Zr_{0.32}O_2$ and $Pt/Ce_{0.5}Zr_{0.5}O_2$) reduce to only two at 18,000 h^{-1}: $Pt/Ce_{0.68}Zr_{0.32}O_2$ and $Pt/Ce_{0.5}Zr_{0.5}O_2$.

4. Conclusions

CO oxidation on $Pt/Ce_XZr_{1-X}O_2$ ($X = 0$, 0.15, 0.5, 0.68, 0.8 and 1) has been studied both in hydrogen-free and hydrogen-rich environment. Those catalysts containing ceria in the support have shown to be robust CO oxidation catalysts, achieving a complete CO oxidation in hydrogen-free streams at temperatures below 112 °C.

Two parameters have been used to correlate catalyst activity in H_2-free streams: support reducibility and Pt content. The former has been quantified by integration of the TPR H_2 uptake until 600 °C, and the best correlation found when expressed in μmol per unit surface area. Use of ceria-containing supports has proven to be a very effective procedure to increase catalyst activity in CO oxidation, although the best behaviour corresponded to catalysts supported on mixed oxides.

Addition of 60 vol.% H_2 to the stream allowed studying PROX, and comparison of the catalyst performance with and without H_2. The presence of H_2 has been shown to shift X_{CO}

curves to lower temperature values, although after a maximum CO conversion is obtained (not necessarily 100%) competence between CO and H_2 for the oxygen produces a decrease of X_{CO} with temperature. A certain excess of oxygen with respect to CO had to be fed to the reaction system in order to reach complete CO conversion in the presence of H_2. For an oxygen excess of $\lambda = 2$, three catalysts were able to reach 100% CO conversion with effective oxygen use: $Pt/Ce_{0.8}Zr_{0.2}O_2$, $Pt/Ce_{0.68}Zr_{0.32}O_2$ and $Pt/Ce_{0.5}Zr_{0.5}O_2$, the latter being the only one to present such behaviour in a significant temperature range.

More demanding conditions of GHSV reduced the adequate catalysts to just two: $Pt/Ce_{0.68}Zr_{0.32}O_2$ and $Pt/Ce_{0.5}Zr_{0.5}O_2$ and even more demanding conditions would seem to reduce the catalysts to just one: $Pt/Ce_{0.5}Zr_{0.5}O_2$. Considering that these catalysts are thought to be used in mobile sources, and the important role of weight and volume reduction in such applications, this catalyst would clearly be the choice.

However, the presence of CO_2 and H_2O in H_2 streams originating from a reforming process is significant, and their effect on catalyst performance was studied by addition of either CO_2 or H_2O to the feedstream. $Pt/Ce_{0.5}Zr_{0.5}O_2$ has been shown to be the only catalyst among the mixed oxides that remains capable of complete CO depletion with effective oxygen use in the presence of either CO_2 or H_2O. However, a new catalyst arises from this study which was not adequate in the absence of CO_2 and H_2O, but is capable of complete CO depletion with effective oxygen use in the presence of these compounds: Pt/CeO_2. More in depth studies should be performed in order to make a choice between these two catalysts, which may depend on the actual application.

Acknowledgements

Authors wish to thank Spanish MEC (project ENE2004-06861) and UPV/EHU (9/UPV-13517) for their financial support.

References

[1] T.V. Choudhary, D.W. Goodman, Catal. Today 77 (2002) 65–78.
[2] A.F. Ghenciu, Curr. Opin. Solid State Mater. 6 (2002) 389–399.
[3] G.J.K. Acres, J.C. Frost, G.A. Hards, R.J. Potter, T.R. Ralph, D. Thompsett, G.T. Burstein, G.J. Hutchings, Catal. Today 38 (1997) 393–400.
[4] W.S. Epling, P.K. Cheekatamarla, A.M. Lane, Chem. Eng. J. 93 (2003) 61–68.
[5] M. Echigo, T. Tabata, Appl. Catal. A-Gen. 251 (2003) 157–166.
[6] S.H. Oh, R.M. Sinkevitch, J. Catal. 142 (1993) 254–262.
[7] A. Manasilp, E. Gulari, Appl. Catal. B-Environ. 37 (2002) 17–25.
[8] M.J. Kahlich, H.A. Gasteiger, R.J.J. Behm, J. Catal. 171 (1997) 93–105.
[9] A. Sirijaruphan, J.G. Goodwin, R.W. Rice, in: Proceedings of the 18th North American Catalysis Society Meeting, Cancún (México), June 1–6, 2003.
[10] M. Echigo, N. Shinke, S. Takami, S. Higashiguchi, K. Hirai, T. Tabata, Catal. Today 84 (2003) 209–215.
[11] D.H. Kim, M.S. Lim, Appl. Catal. A-Gen. 224 (2002) 27–38.
[12] A.K. Santra, D.W. Goodman, Electrochim. Acta 47 (2002) 3595–3609.
[13] K. Arnby, A. Törncrona, B. Andersson, M. Skoglundh, J. Catal. 221 (2004) 252–261.
[14] G. Avgouropoulos, T. Ioannides, C. Papadopoulou, J. Batista, S. Hocevar, H.K. Matralis, Catal. Today 75 (2002) 157–167.
[15] M. Haruta, A. Ueda, S. Tsubota, R.M. Torres-Sánchez, Catal. Today 29 (1996) 443–447.
[16] M. Okumura, J.M. Coronado, J. Soria, M. Haruta, J.C. Conesa, J. Catal. 203 (2001) 168–174.
[17] M. Macieiewski, P. Fabrizioli, J.D. Grundwaldt, O.S. Becker, A. Baiker, Phys. Chem. Chem. Phys. 3 (2001) 3846–3855.
[18] H. Liu, A. Kozlov, A. Kozlova, T. Shido, Y. Iwasawa, Phys. Chem. Chem. Phys. 1 (1999) 2851–2860.
[19] R.J.H. Grisel, B.E. Nieuwenhuys, Catal. Today 64 (2001) 69–81.
[20] D.H. Kim, J.E. Cha, Catal. Lett. 86 (2003) 107–112.
[21] H. Igarashi, H. Uchida, M. Suzuki, Y. Sasaki, M. Watanabe, Appl. Catal. A-Gen. 159 (1997) 159–169.
[22] A.E. Aksoylu, M.M.A. Freitas, J.L. Figueiredo, Catal. Today 62 (2000) 337–346.
[23] M.M. Schubert, M.J. Kahlich, G. Feldmeyer, M. Hüttner, S. Hackenberg, H.A. Gesteigner, R.J. Behm, Phys. Chem. Chem. Phys. 3 (2001) 1123–1131.
[24] X. Liu, O. Korotkikh, R. Farrauto, Appl. Catal. A-Gen. 226 (2002) 293–303.
[25] O. Korotkikh, R. Farrauto, Catal. Today 62 (2000) 249–254.
[26] K. Tanaka, Y. Morooka, K. Ishigure, T. Yajuma, Y. Okabe, Y. Kato, H. Hamano, S. Sekiya, H. Tanaka, Y. Matsumoto, H. Koinuma, H. He, C. Zhang, Q. Feng, Catal. Lett. 92 (2004) 115–121.
[27] M. Shou, K. Tanaka, K. Yoshioka, Y. Morooka, S. Nagano, Catal. Today 90 (2004) 255–261.
[28] A. Sirijaruphan, J.G. Goodwin, R.W. Rice, J. Catal. 224 (2004) 304–313.
[29] I.H. Son, A.M. Lane, Catal. Lett. 76 (2001) 151–154.
[30] J. Yan, J. Cao, P. Li, Catal. Lett. 93 (2004) 55–60.
[31] A. Trovarelli, Catal. Rev. 38 (1996) 439–520.
[32] P. Fornasiero, G. Balducci, R. Di Monte, J. Kašpar, J. Sergo, G. Gubitosa, A. Ferrero, M. Graziani, J. Catal. 164 (1996) 173–183.
[33] J. Kaspar, P. Fornasiero, M. Graziani, Catal. Today 50 (1999) 285–298.
[34] P. Fornasiero, R. di Monte, G.R. Rao, J. Kaspar, S. Meriani, A. Trovarelli, M. Graziani, J. Catal. 151 (1995) 168–177.
[35] C. Descorme, Y. Madier, D. Duprez, J. Catal. 196 (2000) 167–173.
[36] Y. Madier, C. Descorme, A.M. Le Govic, D. Duprez, J. Phys. Chem. B 103 (1999) 10999–11006.
[37] G. Vlaic, P. Fornasiero, S. Geremia, J. Kaspar, M. Graziani, J. Catal. 168 (1997) 386–392.
[38] A. Wootsch, C. Descorme, D. Duprez, J. Catal. 225 (2004) 259–266.
[39] H.S. Roh, H.S. Potdar, K.W. Jun, S.Y. Han, J.W. Kim, Catal. Lett. 93 (2004) 203–207.
[40] A. Cabanas, J.A. Darr, E. Lester, M. Poliakoff, Chem. Commun. (2000) 901–902.
[41] C.E. Hori, H. Permana, K.Y. Simon, A. Brenner, K. More, K.M. Rahmoeller, D. Belton, Appl. Catal. B-Environ. 6 (1998) 105–117.
[42] F.B. Passos, E.R. de Oliveira, L.V. Martos, F.B. Noronha, Catal. Today 101 (2005) 23–30.
[43] F. Fally, V. Perrichon, H. Vidal, J. Kaspar, G. Blanco, J.M. Pintado, S. Bernal, G. Colón, M. Daturi, J.C. Lavalley, Catal. Today 59 (2000) 373–386.
[44] M. Thammachart, V. Meeyoo, T. Risksomboon, S. Osuwan, Catal. Today 68 (2001) 53–61.
[45] M.J. Kahlich, H.A. Gasteiger, R.J. Behm, J. Catal. 171 (1997) 93–105.
[46] S. Johansson, L. Österlund, B. Kasemo, J. Catal. 201 (2001) 275–285.
[47] A. Luengnaruemitchai, S. Osuwan, E. Gulari, Int. J. Hydrogen Energy 29 (2004) 429–435.
[48] T. Bunluesin, R.J. Gorte, G.W. Graham, Appl. Catal. B: Environ. 15 (1998) 107–114.
[49] U. Oran, D. Uner, Appl. Catal. B: Environ. 54 (2004) 183–191.